STRUCTURAL DESIGN AND PERFORMANCE STUDY OF SALT-ALKALI SOIL ROTARY BLADE BASED ON DISCRETE ELEMENTS
/
基于离散元的盐碱地旋耕刀结构设计与性能研究

Shuai ZHENG[1)], Ahmed F. El-SHAFIE[2)], Jie LIU[1)], Abouelnardar SALME[3)], Jing ZHANG[4)] Haoran BAI*[1)]
[1)] College of Mechanical and Electrical Engineering, Qingdao Agricultural University, Qingdao / China;
[2)] National Center of Technology Innovation for Comprehensive Utilization of Saline-Alkali Land, Dongying / China;
[3)] Yellow River Delta Intelligent Agricultural Machinery Equipment Industry Academy, Dongying / China
[4)] Academician Workstation of Agricultural High-tech Industrial Area of the Yellow River Delta,
[5)] Dongying Vocational College School of Ecology and Biology, Dongying / China
Corresponding author: Haoran Bai
Tel: +86-19558970989; E-mail: 20232111061@stu.qau.edu.cn
DOI: https://doi.org/10.35633/inmateh-76-104

Keywords: *rotary blade, saline-alkaline soil, operating power consumption, structural design*

ABSTRACT
Aiming at the issues of high energy consumption and poor tillage quality caused by soil compaction and heavy clay in the saline-alkali soils of the Yellow River Delta, this study systematically analyzes the dynamic interaction between rotary tiller blades and soil, investigates the influence of structural parameters on tillage performance, designs a blade edge curve based on the shearing effect, and identifies the primary factors affecting energy consumption and their respective ranges. Using EDEM software in combination with a quadratic orthogonal rotational combination test, with bending angle, working width, and tangential surface height as the experimental factors and operational power consumption as the evaluation index, the optimal structural parameters were determined through Design-Expert 13 optimization: bending angle of 136.49°, working width of 34.20 mm, and tangential surface height of 42.3 mm, corresponding to a theoretical power consumption of 36.64 kW. Field experiments demonstrated that the designed rotary tiller blade consumed 38.49 kW under the same operating conditions, representing a 16.07% reduction compared with traditional blades, thereby validating the effectiveness of the design. The findings provide a theoretical basis for the utilization of saline-alkali land as well as for resistance reduction and efficiency improvement in rotary tillers.

摘 要
针对黄河三角洲盐碱地土壤板结黏重导致旋耕功耗高、质量差等问题，本文系统分析了旋耕刀-土壤动力学特性，探究旋耕刀结构参数对耕作性能的影响规律，设计了一种基于滑切效果的刃口曲线，明确了影响功耗的主要因素及取值范围。利用EDEM软件和二次正交旋转组合试验，以弯折角、工作幅宽、正切面高度为因素，作业功耗为试验指标，结合Design-Expert 13优化得出最佳结构参数为弯折角136.49°、作业幅宽34.20mm、正切面高度42.3mm，对应理论功耗36.64kW。田间试验表明，所设计旋耕刀在相同工况下功耗为38.49kW，较传统刀具降低16.07%，验证了设计的有效性。研究成果为盐碱地开发利用及旋耕机减阻增效提供了理论依据。

INTRODUCTION
Rotary tillage is the primary cultivation method in the Yellow River Delta region, enabling plowing, efficient soil fragmentation, and land preparation in a single operation. After rotary tillage, the soil surface becomes flat and loose, creating seedbed conditions suitable for sowing, improving soil aeration and water retention capacity, and effectively breaking up and burying crop residues (*Zhao et al., 2025; Liu et al., 2022*). However, compared with other soils, those in this region exhibit high salinity and alkalinity, low organic matter content, and a tendency for underground salts to migrate to the surface, which causes soil hardening and compaction (*Zhu et al., 2024*). As a result, soil fragmentation is poor, and the cutting resistance is high. In practice, rotary tillers often need to rework the soil to achieve the seedbed requirements for sowing, which greatly increases power consumption.

In order to improve the operational efficiency of rotary tillers and reduce blade working resistance, optimizing the geometric structure of rotary tiller blades to reduce power consumption has been an important research direction for scholars in recent years. Recently, the interaction process between rotary tiller blades and soil using the SPH method was simulated, the structural parameters that generate resistance in rotary tiller blades was determined, and their design was optimized.

Time comparison tests showed that the power consumption of the optimized rotary tiller blades was reduced by 9.52%, providing a reference for reducing resistance and saving energy in rotary tiller blades (*Zhang et al., 2024*).

In 2019, a wedge-shaped drag-reducing rotary tiller blade was designed to address the issues of high resistance and energy consumption during rotary tilling operations. Field comparison tests showed that the wedge-shaped rotary tiller blade reduced average torque by 11.35% and average power consumption by 9.29% compared to the national standard rotary tiller blade, effectively reducing tillage energy consumption (*Hao et al., 2019*). By studying the three-directional working resistance experienced by rotary tiller blades and its variation patterns, the experimental factors influencing the three-directional resistance of rotary tiller blades were determined to be the bending angle, blade width, tilling depth, phase angle, and forward speed (*Xiong et al., 2018*).

In 2021, in response to the issues of high resistance and high energy consumption during oilseed rape cultivation, a counter-rotating rotary tiller blade and soil model were established. Through a combination of discrete element simulation and field comparison experiments, the optimal structural parameters of the blade were determined (*He et al., 2022*). In recent years, relevant scholars have studied the impact of the geometric and operational motion parameters of L-shaped rotary tiller blades on the dynamic performance of rotary tillers. They found that changing the sweeper angle can significantly reduce the power consumption of the operation while improving the mixing and burial effect (*Nalawade et al., 2024*).

This paper designs a new type of rotary tiller blade suitable for saline-alkali heavy clay soil. Through kinematic and structural parameter analysis of the rotary tiller blade, a rotary tiller blade-soil dynamic model is constructed. Using EDEM simulation experiments, the study investigated the influence of different structural parameter combinations on operational power consumption. Through orthogonal experiments, the optimal structural parameter combination for the blades was determined. Field comparison experiments were conducted to validate the accuracy of the simulation, aiming to provide references for reducing resistance and improving efficiency in saline-alkali soil cultivation.

MATERIALS AND METHODS

DYNAMIC ANALYSIS AND STRUCTURAL DESIGN OF ROTARY TILLAGE BLADES

Analysis of Rotary Tiller Blade Working Parameters

During rotary tilling operations, the rotary tiller blades rotate around the blade axis center at an angular velocity *ω* while moving forward with the rotary tiller at a linear velocity v_m. Therefore, the absolute motion of the rotary tiller blades is the combination of these two types of motion (*Zhang et al., 2019*). A rectangular coordinate system was established, as shown in Fig. 1, where *O* is the center of rotation of the blade shaft, the positive direction of the *x*-axis is the same as the forward direction of the rotary tiller, and the positive direction of the *y*-axis is perpendicular to the soil surface and downward. The tip of the blade is the point on the blade that can reach the maximum tilling depth. Assuming that the starting position of the blade tip is on the positive *x*-axis, the equation of motion of the blade tip can be expressed as:

$$\begin{cases} x = R\cos\omega t + v_m t \\ y = R\sin\omega t \end{cases} \quad (1)$$

where:

R is the radius of rotation of the blade tip, [mm]; ω - the angular velocity of rotation of the blade shaft, [rad]; v_m - the forward speed of the rotary tiller, [m/s]; t - the operating time, [s].

The end point motion trajectory of the rotary tiller blade is a cycloid. Taking point *A* as either end point of the blade's motion trajectory, the horizontal component velocity v_x and vertical component velocity v_y of point *A* motion are respectively:

$$\begin{cases} v_x = v_m - R\omega\sin\omega t \\ v_y = R\omega\cos\omega t \end{cases} \quad (2)$$

Therefore, the absolute movement speed of the blade tip is:

$$v = \sqrt{v_x^2 + v_y^2} = \sqrt{v_m^2 + R^2\omega^2 - 2v_m R\omega\sin\omega t} \quad (3)$$

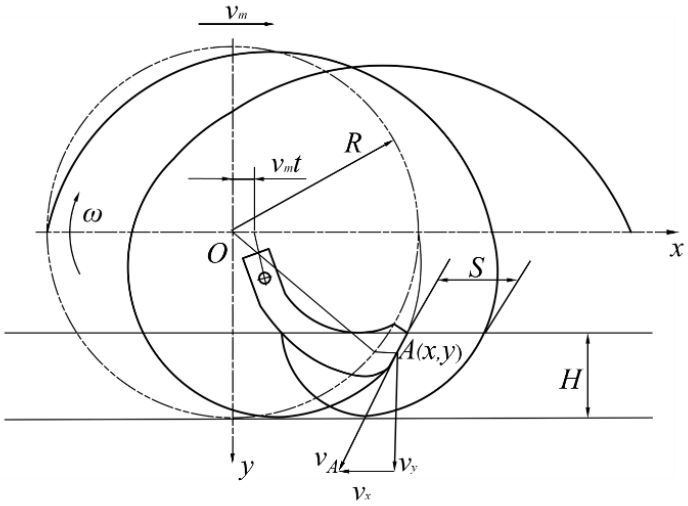

Fig. 1 - Rotary tiller blade working trajectory diagram

Curve Design of Rotary Tiller Blade Edge

When cutting soil, the rotary tiller blade cuts the soil longitudinally with its side cutting edge. Typically, the cutting edge near the center begins to cut the soil, then gradually penetrates the soil from near to far, and finally cuts the soil horizontally with its tangential cutting edge. When designing the cutting edge of a rotary tiller blade, it is important to ensure that the blade curve does not become entangled with grass. The blade should operate according to the principle of sliding achieving the cutting operations, capable of cutting straw or soil clumps with moderate sliding cutting force. If immediate cutting is not possible, the blade should be able to slide along the cutting edge and disengage, preventing grass entanglement and blockages, thereby achieving smooth cutting and minimizing power consumption (*Guan et al., 2021; Zhang et al., 2022*). Therefore, the sliding angle is used as an important basis for the design of the rotary tiller blade edge curve, and the Archimedean spiral is used for the design of the rotary tiller blade edge curve.

Curve Design of Side Cutting Edge of Rotary Tiller Blade

The angle between the velocity vector at a point on the cutting edge of a rotary tiller and the tangent plane of the cutting edge curve at that point, as shown in Fig. 2, is called the slip angle τ at point A on the side cutting edge curve. When the blade rotates only around the blade axis, τ is the static slip angle.

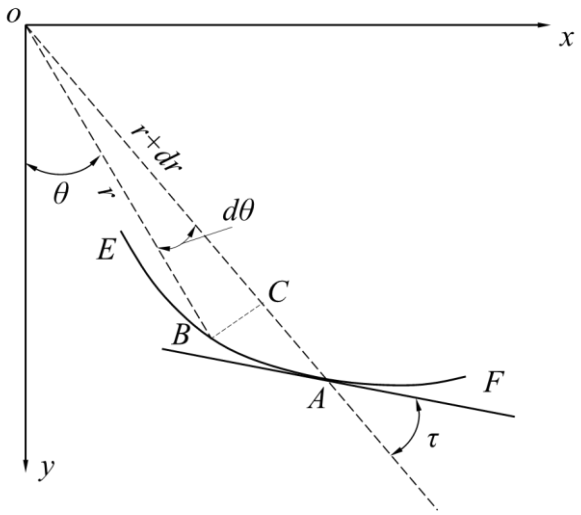

Fig. 2 - Diagram of the sliding cutting action of a rotary tiller blade

Due to the different operating speeds of rotary tillers, the speed direction and magnitude at a point on the side cutting edge curve vary, so the sliding angle value at that point also varies. Therefore, it is necessary to consider the effect of the dynamic sliding angle on the blade. The value of the dynamic sliding angle τ' is (*Liang et al., 2016*):

$$\tau' = \tau - arctan\left(\frac{cos\theta}{\lambda\frac{r}{R} - sin\theta}\right) \quad (4)$$

where: θ is the polar angle, [rad]; λ is the rotary tiller speed ratio.

The Archimedes spiral line has the characteristic of gradually increasing sliding cutting action, cutting soil from near to far. The feed rate of the blade in the radial direction is uniform, thereby achieving reasonable load distribution and stable operation (*Zhang et al., 2023*). Therefore, the Archimedes spiral line is used as the side cutting edge curve design of the rotary tiller blade. The Archimedean spiral equation for the design is:

$$r = r_0 + \Delta r\theta \quad (5)$$

where: r_0 is the initial polar radius, [mm]; Δr - the increase in the polar radius *r,* when the helix increases by 1rad, [mm].

The initial radius r_0 of the side cutting edge is one of the basic parameters for designing a rotary tiller blade. Based on the current status of rotary tillage in saline-alkali soil and the agronomic requirements for sowing subsequent crops, the tillage depth H is set to 120 mm to ensure stable tillage. The maximum radius of rotation R of the blade is set to 195 mm. According to the Agricultural Machinery Design Manual, when the soil is highly viscous and has a low moisture content, the cutting pitch S can be set to 60-90 mm. To ensure effective soil fragmentation, the cutting pitch should not be too large. It can be appropriately reduced to improve soil fragmentation.

The cutting pitch S is set to 80 mm.

$$r_0 = \sqrt{R^2 + S^2 - 2S\sqrt{2RH - H^2}} \quad (6)$$

Substituting the design values of R, H, and S into equation (6) yields an initial polar radius r_0 of 125 mm for the side cutting edge curve. To ensure that the side cutting edge curve transitions smoothly with the tangential cutting edge, thereby achieving a smooth soil penetration effect, the r_1 value is generally 10-20 mm smaller than the rotational radius R of the rotary tiller blade. In this case, it is set to 185 mm. The extreme angle θ_1 at the end of the cutting edge curve is:

$$\theta_1 = \frac{r_1 - r_0}{r_1} tan\tau_1 \quad (7)$$

where:

τ_1 is the static shear angle at the end of the side cutting edge curve, [°].

The size of the sliding angle is directly related to the resistance of the operation. If it is too large, it will increase the power consumption of the operation; if it is too small, it will not be possible to push soil clumps and straw out of the cutting edge. Considering the saline-alkali soil operating environment, the static sliding angle τ_1 at the endpoint of the cutting edge curve is designed to be 60°. Then, the terminal extreme angle θ_1 is 0.56 rad. From equation (5), it can be seen that the independent parameters include the polar radius r_0 of the starting point of the cutting edge curve and the polar radius increment Δr. Given the initial polar radius r_0 and the terminal polar radius θ_1 of the cutting edge curve of the rotary tiller, the above parameters can be substituted into equation (8).

$$\Delta r = \frac{r_1 - r_0}{\theta_1} \quad (8)$$

The increase in the helix angle Δr is 1.87, at which point the side cutting edge of the rotary tiller blade is:

$$r = 125 + 1.87\theta \quad (9)$$

Analysis of Rotary Tiller Blade Structural Parameters

Based on the analysis of the rotary tiller blade curve described above, a new rotary tiller blade was designed using the constructed curve. Its structural parameters are shown in Fig. 3.

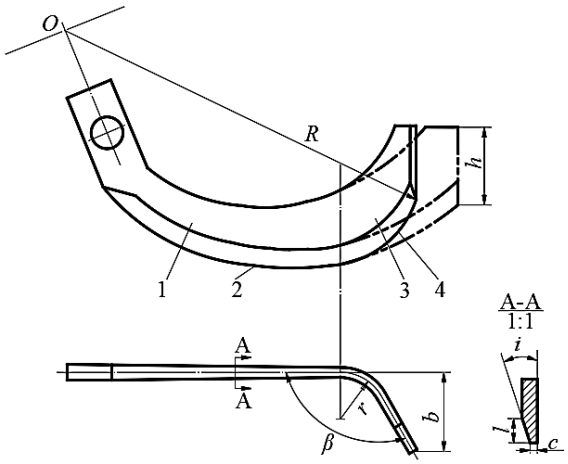

Fig. 3 - Diagram of the sliding cutting action of a rotary tiller blade

1 - side cutting surface; 2 - side cutting edge; 3 - tangential cutting surface; 4 - tangential cutting edge; R - blade rotation radius; h - tangential cutting surface height; β - bending angle; r - bending radius; b - working width; l - cutting edge width; c - cutting edge thickness.

Rotary tiller blade structural parameter design:

1. Blade rotation radius R. The design of the rotation radius R is based on factors such as working depth and soil properties. A larger rotation radius increases the working range of the blade, improving working efficiency, but also increases working resistance and power consumption; a smaller rotation radius helps reduce energy consumption and is suitable for harder soils, but may affect soil fragmentation effectiveness. Based on the designed working depth H = 120 mm in this paper, the blade rotation radius R = 195 mm is selected in this design (*Qin et al., 2021*).

2. Tangential height h. When the tangential height of the rotary tiller blade is too small, the quality of soil tossing and soil fragmentation deteriorates, and it cannot meet the requirements of agricultural cultivation. When the tangential height of the rotary tiller blade is too large, the tilling resistance of the rotary tiller blade increases, and the bent section is prone to breakage. Referring to relevant research content and combining the saline-alkali soil working environment, the tangential height is selected to be 35-65 mm (*He et al., 2021*).

3. Bending angle *β*. The angle formed between the tangential surface and the lateral surface of the rotary tiller blade after bending. If the bending angle of the rotary tiller blade is too large, the tip of the tangential blade will first come into contact with the soil and straw, increasing tillage resistance and reducing the service life of the tillage blade. If the bending angle is too small, the bent portion of the tillage blade will first contact the soil, resulting in better sliding cutting performance, but it will increase the contact area between the tangential surface and the soil, thereby increasing cutting resistance. According to the requirements for reducing resistance and combining operational requirements, a bending angle of 115° to 145° should be selected (*Xiao et al., 2024*).

4. Working width b. When the working width of the blade is too large, it will increase the resistance of single-blade operation. When the working width is too small, it will affect the quality of cultivation. Therefore, under the premise of meeting agronomic requirements, the working width *b* of the blade should be selected as 35-55 mm (*Yang et al., 2024*).

Based on the above analysis, the key parameters affecting the cutting resistance of rotary tiller blades in their structural design are the bending angle *β*, tangential height *h*, working width *b*, and rotational radius R, which have a significant impact on the operational performance of rotary tiller blades. Among them, the turning radius R has been determined. Changes in the bending angle *β*, tangential height *h*, and working width *b* have a direct impact on the power consumption and quality of rotary tillage operations. Therefore, these three parameters were selected as experimental factors. Combined with the requirements for preparing seedbeds in saline-alkali soil, a second-order orthogonal rotated center combination experiment was conducted on the three experimental factors to determine the optimal combination parameters and further analyze the power consumption during rotary tillage operations.

ESTABLISHMENT OF DISCRETE ELEMENT MODELS

Soil Model Settings

This experiment was conducted at the Agricultural Experiment and Demonstration Base for Saline-Alkali Land in the Yellow River Delta Agricultural High-Tech Industrial Demonstration Zone in Shandong Province. Using EDEM software, a soil discrete element model was established. The soil particle contact model selected was Hertz-Mindlin with Bonding, which can simulate the bonding action of soil particles, forming bonding action between particles until the limit of bonding rupture is reached (*Makange et al., 2020; Asl et al., 2020*).

The soil particle radius was set to 5 mm. The particle bonding radius is calculated based on soil density and moisture content. The rotary tiller blades are made of 65 Mn steel. To simulate actual working conditions, the forward speed is set to 1.38 m/s, the rotation speed to 330 r/min, and a tillage depth of 12 cm. A soil trench with dimensions of (length × width × height) 2000 mm × 1100 mm × 400 mm was established in the model, and a particle factory was set up above the soil trench to generate 401,800 soil particles using the gravity deposition method. The particles were bonded together via linking bonds, and the simplified rotary tiller blade model was imported. Simulation parameters were selected based on preliminary studies of the mechanical properties and contact parameters of saline-alkali soil, and the intrinsic parameters and contact parameters of each material required for the simulation model were determined through experiments (*Mak et al., 2012; Wang et al., 2024; Xu et al., 2025*). The simulation contact model parameters and simulation contact parameters are shown in Tables 1 and 2.

Table 1

Simulation model parameters

Materials	soil	65Mn
Density [kg·m^{-3}]	1.58×10^{3}	7.85×10^{3}
Poisson's ratio	0.32	0.30
Shear modulus [Pa]	7.25×10^{6}	7.90×10^{9}

Table 2

Simulated contact parameters

Materials	soil
Soil-soil recovery factor	0.35
Soil-soil static friction factor	0.5
Soil-soil rolling-friction facto	0.15
Soil-steel recovery factor	0.3
Soil-steel static friction factor	1.15
Soil-steel rolling friction factor	0.15
Normal rigidity [N·m^{-3}]	5×10^{8}
Tangential rigidity [N·m^{-3}]	5×10^{8}
Critical normal stress [Pa]	3×10^{6}
Critical tangential stress [Pa]	3×10^{6}

Experimental Design

Based on the above research, this experiment selected X1 bend angle, X2 tangent plane height, and X3 working width as experimental factors. According to the analysis of the experimental factors mentioned above, the bending angle was set at 115-145°, the tangent surface height at 35-65 mm, and the working width at 34-56 mm. An orthogonal rotation center combination experiment was conducted, and the experimental factor codes are shown in Table 3.

Table 3

Experimental factors and level coding

code	factors		
	X1	X2	X3
-1.353	110	30	30
-1	115	35	34
0	130	50	45
1	145	65	56
1.353	150	70	60

During the process of rotary tillage blades cutting soil, according to the principles of theoretical mechanics, changes in the torque of the blade shaft can reflect power consumption. Power consumption during rotary tillage operations can be calculated using equation (10).

$$P = \frac{n}{9550} \times M \tag{10}$$

where:

P is the power consumption, [kW]; n is the blade shaft speed, [r/min]; M is the blade shaft torque, [N·m].

Therefore, during rotary tilling operations, simply recording the torque and rotational speed of the blade shaft allows for the calculation of power consumption by the rotary tilling blades during operation.

RESULTS

Simulation Process Analysis

The total simulation duration is set to 3 seconds, with 0-1 seconds designated as the particle generation time and 1.1 seconds as the start time for the rotary tiller blade movement. A fixed time step size of 10% is set, and the grid size is set to 2.5 times the average particle radius, which corresponds to Rayleigh's value of 8.56e+10^{-6}. Data is saved every 0.01 seconds. The simulation model is shown in Fig. 4.

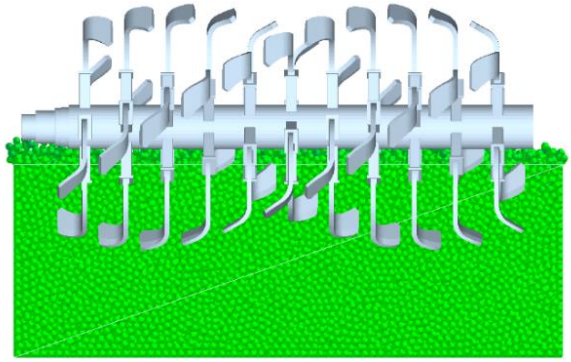

Fig. 4 - Rotary tiller blade - Discrete element simulation model for saline-alkali soil

During the simulation process, the torque applied to the rotary tiller blade shaft is recorded to calculate the power consumption of the rotary tiller during operation. The power consumption curve during the rotary tilling process is shown in Fig. 5.

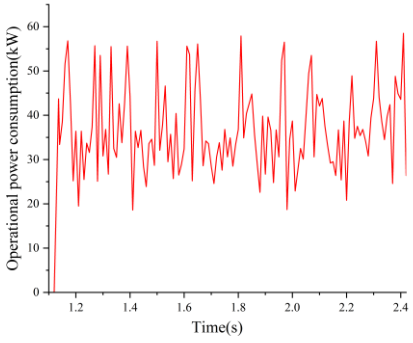

Fig. 5 - Power consumption curve diagram for rotary tiller operation

In the rotary blade simulation process, EDEM simulation post-processing can be used to analyze the dynamic contact process between the blade and the soil at different times, as shown in Fig. 6. As the blade shaft continues to move forward, the side cutting edge of the rotary tiller blade first contacts and cuts into the uncultivated soil in front of it. Under the combined action of cutting force and thrust, the soil particles accelerate. The tangential surface area of the blade forms a localized high-speed soil ejection zone. Soil particles are subjected to intense disturbance under the movement of the blade, moving backward and forward in a projectile-like manner, and the soil particles appear red in color. Overall, the velocity vectors of soil particles exhibit distinct layered characteristics. Particles at the leading edge of the blade move violently, primarily consisting of soil fragmentation and ejection movements. Particles below the blade move slowly, primarily involving compression and shear movements. Therefore, under the reciprocating action of the rotary tiller blade, soil particles are both disrupted and ejected, completing the entire cutting process. At the same time, the movement of soil particles also reflects the soil cutting mechanism of rotary tillers in actual operation and indicates that blade structural parameters have a significant impact on soil disturbance and energy consumption.

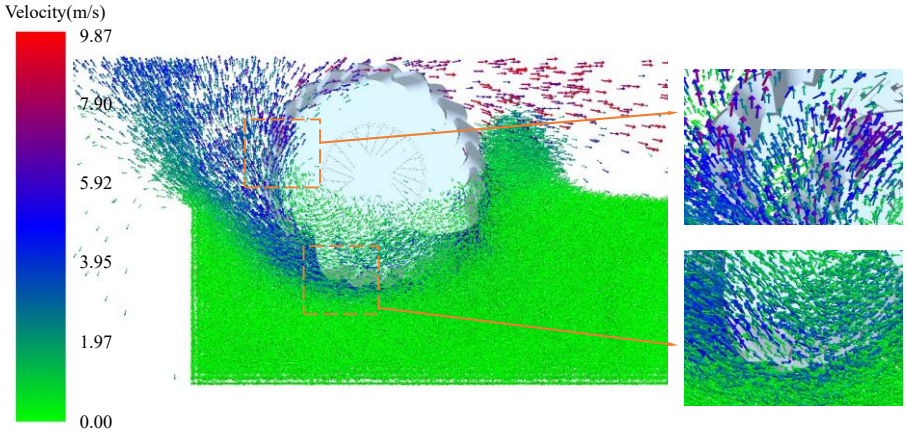

Fig. 6 – Rotary tiller cutting operation vector diagram

Through 17 simulation tests on EDEM, with bending angle, tangent height, and working width as test factors, and operating power consumption Y as the evaluation index, the measurement results are shown in Table 4.

Table 4

Experimental Results

Number	Factor			Operating power consumption Y [kW]
	X1 [°]	X2 [mm]	X3 [mm]	
1	-1	-1	-1	43.6
2	1	1	-1	36.8
3	-1	1	-1	53.5
4	1	-1	-1	39.8
5	-1	-1	1	44.8
6	1	1	1	42.7
7	-1	1	1	58.6
8	1	0	1	47.6
9	-1.353	0	0	52.4
10	1.353	-1.353	0	39.4
11	0	1.353	0	38.6
12	0	0	0	47.2
13	0	0	-1.353	38.8
14	0	0	1.353	45.3
15	0	0	0	40.8
16	0	0	0	40.6
17	0	-1	0	41.5

Analysis of Test Results

The test results were analyzed using Design-Expert 13 software to perform significance tests and variance analysis on the experimental data in Table 4, yielding the significance test results for the Y power consumption regression model in Table 5. As shown in Table 5, the analysis of operational power consumption $Y1$ indicates that at the P < 0.05 significance level, $X1$, $X2$, $X3$, $X1X2$, $X1^2$ and $X2^2$ are highly significant model terms; $X1X3$, $X2X3$, and $X3^2$ for significant model terms. The overall model P-value and coefficient of determination R^2 are <0.0001 and 0.9932, respectively, while the P-value for the non-significant terms is 0.2610. This indicates that the model is highly significant and has a very high fitting accuracy, with the non-significant terms not being statistically significant, and the regression being valid. The regression equation for operational power consumption Y is obtained.

$$Y = 40.78 - 4.39X1 + 3.71X2 + 2.47X3 - 1.98X1X2 + 0.9250X1X3 + 0.7250X2X3 + 2.93X1^2 + 1.29X2^2 + 0.8226X3^2 \quad (11)$$

Table 5

Analysis of variance of power consumption Y

Source	Sum of Squares	Freedom	Mean Square	F	P-Value
Model	571.38	9	63.49	113.36	<0.0001**
X1	224.70	1	224.70	401.21	<0.0001**
X2	160.30	1	160.30	286.22	<0.0001**
X3	71.10	1	71.10	126.95	<0.0001**
X1X2	31.20	1	31.20	55.72	0.0001**
X1X3	6.85	1	6.85	12.22	0.0100*
X2X3	4.21	1	4.21	7.51	0.0289*
$X1^2$	57.38	1	57.38	102.45	<0.0001**
$X2^2$	11.10	1	11.10	19.82	0.0030**
$X3^2$	4.54	1	4.54	8.10	0.0248*
Residual	3.92	7	0.5601		
Lack of Fit	3.47	5	0.6948	3.11	0.2610
Pure Error	0.4467	5	0.2233		
Cor Total	575.30	16			

Note: * indicates a significant effect (P<0.05), ** indicates a highly significant effect (P<0.01).

Response Surface Analysis

The response surface plots of the operating power consumption for any two factors, namely the bending angle, tangential height, and working width, as interaction factors are shown in Fig. 7.

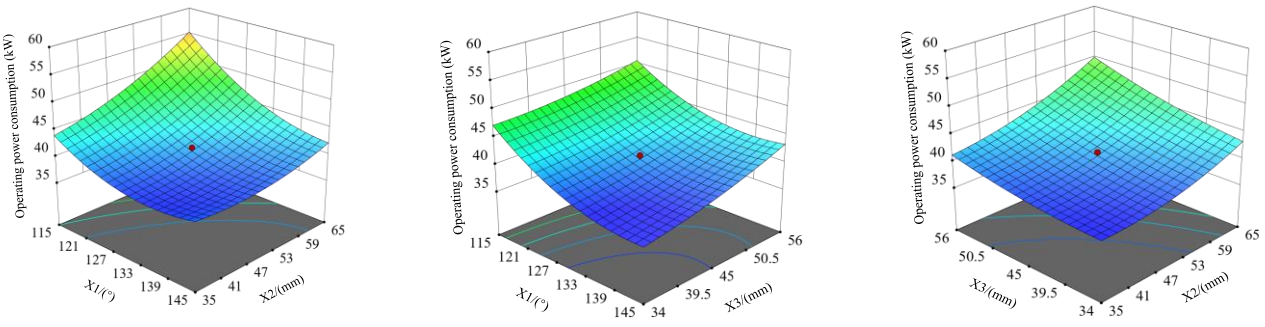

(a) The interaction of X1 and X2 factors *(b) The interaction of X1 and X3 factors* *(c) The interaction of X2 and X3 factors*

Fig. 7 - Response surface analysis of power consumption during rotary tillage

As shown in Fig. 7a, when the working width is at the zero level, the operational power consumption increases as the bending angle decreases and the tangential height increases. As shown in Fig. 7b, when the tangential surface height is at the zero level, the operational power consumption decreases as the working width decreases and the bending angle increases. Additionally, the operational power consumption changes more rapidly with the direction of the bending angle than with the direction of the working width.

Therefore, during rotary tillage operations, the bending angle has a greater influence on operational power consumption than the working width. As shown in Fig. 7c, when the bending angle is at the zero level, the operational power consumption increases with the increase in working width and tangential surface height.

As shown in Table 5, the F values in the table indicate the influence of each influencing factor on the test indicators. The larger the F value, the greater the influence on the test indicators. The degree of influence of each test factor on the operational power consumption Y, from greatest to least, is as follows: $X1$ bend angle, $X2$ tangential face height, and $X3$ working width.

Optimal Design of Experimental Combinations

To determine the optimal combination of rotary tiller blade parameters while ensuring rotary tilling quality, an optimization design was conducted for each experimental factor. By combining the boundary conditions of each factor, the goal of reducing blade cutting resistance and improving rotary tilling quality was achieved. The objective function and constraint function were determined as follows:

$$\begin{cases} Y_{min} \\ s.t. \begin{cases} 110° \le X1 \le 150° \\ 30mm \le X2 \le 70mm \\ 30mm \le X3 \le 60mm \end{cases} \end{cases} \quad (12)$$

Using Design-Expert 13 software for analysis and solution, the optimal parameter combination affecting the power consumption of the operation was obtained as follows: bending angle 136.49°, working width 34.20 mm, and tangent height 42.23 mm. At this point, the power consumption of the operation was 36.64 kW. To verify the accuracy of the optimization results, performance verification tests were conducted on the optimized rotary tiller blades. Three measurements were taken and averaged, resulting in an average operating power consumption of 37.48 kW. The test results show that the maximum error between the theoretical value and the test value is 2.24%. The simulation test results are basically consistent with the theoretical results, indicating that the regression equation is accurate.

Results validation

The experimental field is located at the Saline-Alkali Land Agricultural Experiment and Demonstration Base in the Yellow River Delta Agricultural High-Tech Industrial Demonstration Zone, Dongying City, Shandong Province (118°65E, 38°32′N). It has a warm temperate semi-humid monsoon climate with distinct seasons, an annual average temperature of 12.3°C, an annual average precipitation of 587.4 mm, an annual average sunshine duration of 2,234 hours, and a frost-free period of 198 days. The soil at this experimental base is coastal saline-alkali soil, with soil salinity levels ranging from 1‰ to 10‰, encompassing three categories of saline-alkali land: mild, moderate, and severe. This experiment was conducted on mild saline-alkali land.

Field Trial Conditions

During field trials, the test field was divided into five plots, each 50 m long and 1.5 times the width of the machinery. The first 10 m of each plot was designated as the acceleration zone for the machinery, and the middle 20 m was designated as the stable forward movement zone for the machinery. The testing equipment primarily includes a Deutz-Fahr 1804 tractor, a rotary tiller prototype, a ring blade, a measuring tape (3m), steel ruler (300 mm), electronic scale, sealed bags, tape measure (50 m), 0.5 m × 0.5 m square frame, TOP CLOUD-AGRI TECHNOLOGY CO (TJSD-750-II) soil compaction meter, and TOP CLOUD-AGRI TECHNOLOGY CO (TZS-1K-G) soil moisture rapid tester.

The working environment conditions during field trials are shown in Table 6. During field trials, the testing methods for machinery are based on NY/T499-2013 “Rotary Tiller Operational Quality” and GB/T5668-2017 “Rotary Tiller,” with operational power consumption as the testing criterion. Power consumption was measured using an HCNJ-101 dynamic torque sensor (torque range: 0.05-2000 N·m; speed range: 2000 r/min) and a three-point tension sensor (SBT620TF-10T). The field test process is shown in Fig. 8.

Table 6

Test environmental characteristics

Measurement item	Argument
Soil moisture content [%]	18.58
Volume weight of soil [g·cm^{-3}]	1.45
Soil compactness [kg/cm^2]	26.72
Soil pH value	7.86

(a) Rotary tiller operation diagram *(b) Torque sensor installation diagram*

Fig. 8 – Field trial effect diagram

Analysis of Field Trial Results

During field trials, the designed rotary tiller blades were compared with traditional rotary tiller blades (GB/T 5669-2017 Rotary Tiller Blade IIT195, bending angle 120°, tangential surface height 50 mm, working width 50 mm) for experimental comparison. Due to the complex field conditions of saline-alkali soil, there was a certain degree of error between the experimental results and the simulation values. Therefore, the power consumption data from five tests within the specified time period were recorded, and their average value was taken as the experimental measurement result. Under identical initial simulation parameters (i.e., bending angle of 136.49°, working width of 34.20 mm, and tangential height of 42.23 mm), the measured average power consumption of the rotary tiller was 38.49 kW, which resulted in a measurement error of 4.81 % compared to the simulated average power consumption of 36.64 kW. Further validation of simulation accuracy is provided by the field test results shown in Table 7. The actual test values are higher than the simulation test values, consistent with the results obtained by other scholars in soil shear tests (*Kang et al., 2016*).

Table 7

Field trial comparison results

Serial number	Design of rotary blades		Traditional rotary blade	
	torque value M [Nm]	Operating power consumption Y [kW]	torque value M [Nm]	Operating power consumption Y [kW]
1	1103.45	38.13	1254.16	43.34
2	1094.06	37.81	1308.64	45.22
3	984.35	34.01	1322.73	45.71
4	1147.62	39.66	1426.18	49.28
5	1238.73	42.86	1324.37	45.76
Average	1113.64	38.49	1327.22	45.86

As shown in the experimental results of Table 8, the maximum power consumption value of the designed rotary tiller blade during field operations was 42.86 kW, the minimum was 34.01 kW, and the average was 38.49 kW. The error between the simulated values and the theoretical values was less than 10%, indicating that the simulated power consumption has high accuracy.

Under the same operational conditions, the power consumption of the traditional rotary tiller blade ranged from a maximum of 49.28 kW to a minimum of 45.22 kW, with an average value of 45.86 kW. Compared to the results of the traditional rotary tiller blade, the power consumption of the designed rotary tiller blade during operation was reduced by 16.07%. The results indicate that by optimizing the structural parameters of the rotary tiller blade, the resistance during operation can be effectively reduced.

CONCLUSIONS

1) In response to the high energy consumption and poor quality of rotary tillage operations caused by the compacted and heavy soil in the saline-alkali lands of the Yellow River Delta, this paper systematically analyzes the dynamic characteristics of rotary tillage blades and soil, investigates the influence of rotary tillage blade structural parameters on the tillage performance of saline-alkali soils, and designs a blade edge curve based on the sliding cutting effect. It clarifies that the bending angle, tangent plane height, and working width are the primary factors influencing operational energy consumption.

2) Through orthogonal center combination experiments and discrete element simulation analysis, the optimal parameter combination was obtained: bending angle 136.49°, working width 34.20 mm, tangent height 42.23 mm, corresponding to an operating power consumption of 37.80 kW. Performance verification tests showed that the maximum error between the theoretical value and the test value was 2.24%, and the regression model was accurate.

3) Field comparison tests showed that under conditions of soil hardness of 26.72 kg/cm², moisture content of 18.58%, and pH value of 7.86, the average power consumption of the designed rotary blade was 38.49 kW. Compared with traditional rotary blade, power consumption is reduced by 16.07%, meeting the requirements for tilling heavy, sticky soil on saline-alkali land. This provides theoretical reference for the development of saline-alkali land and the optimization of rotary tillers.

ACKNOWLEDGEMENT

This research is supported by the National Key Research and Development Program of China (Project no. 2023YFD2001400); Shandong Province Key Research and Development Program (Science and Technology Demonstration Project): Creation and Industrial Application of Fertilizer and Intelligent Equipment for Improving the Fertility of Saline-Alkali Soil (2024SFGC0405); National Key R&D Program of China (Project no.2022YFE0125800); Development of Key Components for High-Efficiency Tillage Equipment for Saline-Alkali Soil (Y20240055); Research and Development of High-Quality Tillage and Composite Operations Technology and Equipment for Saline-Alkali Land (WSR2023093).

REFERENCES

[1] Asl, J. H., & Singh, S. (2009). Optimization and evaluation of rotary tiller blades: Computer solution of mathematical relations. *Soil and Tillage Research*, *106*(1), 1-7. https://doi.org/10.1016/j.still.2009.09.011

[2] Guan C. (2021). *Basic Research on the Layered Tillage Technology by biaxial rotary tillage component for vegetable bed former (双轴分层旋耕碎土起垄技术基础研究)*. [Doctoral dissertation, Jiangsu University]. https://link.cnki.net/doi/10.27170/d.cnki.gjsuu.2021.000032. Jiangsu/China

[3] Guan, C., Fu, J., Cui, Z., Wang, S., Gao, Q., & Yang, Y. (2021). Evaluation of the tribological and anti-adhesive properties of different materials coated rotary tillage blades. *Soil and Tillage Research*, *209*, 104933.

[4] Hao J., Yu H., Zhao J., Li J., Ma Z., & Cai J. (2019). Design and test of wedge drag reduction rotary blade (楔形减阻旋耕刀设计与试验). *Transactions of the Chinese Society of Agricultural Engineering (Transactions of the CSAE)*, 35(8): 55-64. Hebei/China.

[5] He X., Zhang X., Zhao Z., Shang S., Wang D., & Yang S. (2022). Design and optimization tests of reverse spin-throwing cyperus edulis starting device (反向旋抛式油莎豆起挖装置设计与试验). *Transactions of the Chinese Society for Agricultural Machinery*, 53(05), 34-43. Wulumuqi/China

[6] He X., Zhang X., Zhao Z., Shang S., Wang D., & Yuan X., (2021). Design and test of resistance-reducing excavation device of Cyperus edulis based on discrete element method (基于离散元法的油莎豆降阻挖掘装置设计与试验). *Transactions of the Chinese Society for Agricultural Machinery*, 52(12), 124-133. doi:10.6041/j.issn.1000-1298.2021.12.013. Wulumuqi/China

[7] Kang J., Li S., Yang X, & Liu L. (2016). Structure parameters optimization of sine exponential curve type ditching blade (正弦指数曲线型开沟刀片结构参数优化). *Transactions of the Chinese Society for Agricultural Machinery*, 47(11), 91-99+17. doi:10.6041/j.issn.1000-1298.2016.11.012. Beijing/China

[8] Liang F., Wang D. C., You Y., Wang G., Zhang X., He C. B., & Li S. (2016). Design and optimization of the edge curve of root-cutting blade in grassland (草地破土切根刀具的刃口曲线设计与优化). *Journal of China Agricultural University*, 21(06),100-107. Beijing/China

[9] Liu G., Xia J., Zheng K., Cheng J., & Wei Y. (2022). Design and experiments of the barrier type rotary anti-adhesion blade roller with vibration crosspiece (振动横挡阻隔式旋耕防粘结刀辊设计与试验). *Transactions of the Chinese Society of Agricultural Engineering*. Vol. 38(23), pp. 29-40. Wuhan/China

[10] Makange, N. R., Ji, C., & Torotwa, I. (2020). Prediction of cutting forces and soil behavior with discrete element simulation. *Computers and Electronics in Agriculture*, *179*, 105848. https://doi.org/10.1016/j.compag.2020.105848

[11] Mak, J., Chen, Y., & Sadek, M. A. (2012). Determining parameters of a discrete element model for soil–tool interaction. *Soil and Tillage Research*, *118*, 117-122. https://doi.org/10.1016/j.still.2011.10.019.

[12] Nalawade, R. D., Singh, K. P., Roul, A. K., Agrawal, K. N., Sonawane, S., Mahore, A., & Elbeltagi, A. (2024). Study on the effect of geometrical and operational parameters on performance dynamics of modified rotary blades using DEM. *Scientific Reports*, 14(1), 19239. https://doi.org/10.1038/s41598-024-69803-8

[13] Qin K., Liang X., Cao C. M., Ding W., Wu Z., & Fang L. (2021). Design and experiment of combined cutting and throwing ditching blade for tea garden (茶园切抛组合式开沟刀设计与试验). *Transactions of the Chinese Society for Agricultural Machinery*, 52(05), 74-82. Anhui/China

[14] Wang D., Lu T., Zhao Z., Shang S., Zheng S., & Liu J. (2024). Calibration of discrete element simulation parameters for cultivated soil layer in coastal saline alkali soil (滨海盐碱地耕作层土壤离散元仿真参数标定方法). *Transactions of the Chinese Society for Agricultural Machinery*, 55(11),240-249. https://link.cnki.net/urlid/11.1964.S.20240903.1531.002. Qingdao/China

[15] Xiong P., Yang Z., Sun Z., Zhang Q., Huang Y., & Zhang Z. (2018). Simulation analysis and experiment for three-axis working resistances of rotary blade based on discrete element method (基于离散元法的旋耕刀三向工作阻力仿真分析与试验). *Transactions of the Chinese Society of Agricultural Engineering (Transactions of the CSAE)*, 34(18): 113-121. doi: 10.11975/j.issn.1002-6819.2018.18.014. Guangzhou/China

[16] Xiao W., Niu, Wang P., Xie Y., Xia F. (2024). Simulation ANSYS and optimization of soil cutting of rataty blade by ANSYS/LS-DYNA (基于 ANSYS/LS-Dyna 旋耕刀切土仿真分析及优化). *INMATEH-Agricultural Engineering*, 72(1):22-32. DOI: https://doi.org/10.35633/inmateh-72-02

[17] Xu, N., Xin, Z., Yuan, J., Gao, Z., Tian, Y., Xia, C., Liu, X., & Wang, D. (2025). Calibration of Discrete Element Simulation Parameters and Model Construction for the Interaction Between Coastal Saline Alkali Soil and Soil-Engaging Components. *Agriculture*, 15(1), 7. https://doi.org/10.3390/agriculture15010007

[18] Yang D., Cai W., Wu R., Zhang X., He Y., He L., & Xiong A. (2024). Optimization design of rotary cultivator blade structure parameters for tea garden micro-tillers based on discrete element method (基于离散元法茶园微耕机旋耕刀结构参数优化设计). *Southern Agricultural Machinery*, 55(01),7-10+15. doi:10.3969/j.issn.1672-3872.2024.01.002. Nanchang/China

[19] Zhao, Z., Hou, J., Guo, P., Xia, C., Yan, H., & Wang, D. (2025). Analysis of Soil–Straw Movement Behavior in Saline–Alkali Soil Under Dual-Axis Rotary Tillage Based on EDEM. *Agriculture*, *15*(3), 337.

[20] Zhu, W., Gu, S., Jiang, R., Zhang, X., & Hatano, R. (2024). Saline–alkali soil reclamation contributes to soil health improvement in China. *Agriculture*, *14*(8), 1210.

[21] Zhang X., Hu X., Zhang L. & Kheiry A. (2024). Simulation and structural parameter optimization of rotary blade cutting soil based on SPH method. *International Journal of Agricultural and Biological Engineering*, 17(3):82-90. doi: 10.25165/j.ijabe.20241703.8470.

[22] Zhang C., Xia J., Zhang J., Zhou H., Zhu Y., & Wang J. (2019). Design and experiment of knife roller for six-head spiral straw returning cultivator (六头螺旋秸秆还田耕整机刀辊设计与试验). *Transactions of the Chinese Society for Agricultural Machinery*, 50(3):25-34. https://doi:10.6041/j.issn.1000-1298.2019.03.003. Wuhan/China

[23] Zhang, X., Zhang, L., Hu, X., Wang, H., Shi, X., & Ma, X. (2022). Simulation of soil cutting and power consumption optimization of a typical rotary tillage soil blade. *Applied Sciences*, *12*(16), 8177.

[24] Zhang Q.S., Qi T., Ao Q., Shu C. X., Liao Y., & Liao Q. (2023). Design and experiment of rapeseed direct seeding machine with furrow opener and shallow plowing (油菜机械直播机开沟浅旋装置设计与试验). *Transactions of the Chinese Society for Agricultural Machinery*, 54(10), 58-67+104. doi:10.6041/j.issn.1000-1298.2023.10.005. Wuhan/China